COMPUTED WATER CIRCULATION OF LAKE ONTARIO

FOR OBSERVED WINDS FROM 20 APRIL TO 14 MAY, 1971

by

T. J. Simons and D. E. Jordan

June, 1972

Canada Centre for Inland Waters

Burlington, Ontario

TABLE OF CONTENTS

1. DESCRIPTION OF EXPERIMENT

In a previous paper (Simons, 1971a) a numerical model has been presented for the computation of the water movements in the Great Lakes under homogeneous conditions. The model was applied to Lake Ontario and various results of computations pertaining to the response of the lake to idealized wind stresses were discussed. The present report is devoted to computations of the response of Lake Ontario to actual wind forcing as derived from wind observations on the lake. The particular experiment to be described covers the period from April 20 to May 14, 1971. Also included is a discussion of the implications of the computed circulations with regard to the dispersion of dissolved or suspended matter in the lake.

Three meteorological buoy systems were deployed in Lake Ontario by the Canada Centre for Inland Waters for the period April 19 to October 15, 1971. A description of the buoy experiment has been presented by Taylor (1971) and the positions of the buoys are shown in Figure 1. The wind data recorded at 10-minute intervals were averaged to obtain hourly mean values. Furthermore, since the stations were restricted to the western end of the lake, the hourly averages from all recorders were combined to give one representative mean wind for western Lake Ontario. No attempt was made to determine

the spatial variation of the wind field over the whole lake area. Instead, a spatially uniform wind stress was applied as derived from the above mean wind. This procedure should be acceptable to obtain a first estimate of the reaction of the lake to a realistic time-dependent wind forcing.

The wind stress components to the East (τ_e) and to the North (τ_n) were computed from the wind components by the relationships

$$\tau_e/\rho = -C_D W_e \sqrt{W_e^2+W_n^2} \qquad \tau_n/\rho = -C_D W_n \sqrt{W_e^2+W_n^2} \qquad (1)$$

where W_e and W_n are the eastwind and northwind, respectively, and the minus sign takes care of the meteorological conventions regarding wind directions. The coefficient C_D (which includes the density ratio of air to water) was assigned a value of $1.5\ 10^{-6}$ based on most recent observations on Lake Ontario (F. Elder, personal communication).

The present computations include the hydraulic circulation associated with the discharges of the Niagara River and the St. Lawrence. These discharges are quite variable as seen from the following data published by the Water Survey of Canada (1970). The units are 1000 cubic feet per second = $2.8317\ 10^7$ cm^3/sec.

Table 1: Discharges of Niagara River and St. Lawrence River

	Niagara		St. Lawrence	
Observation period	41 years	1967	9 years	1967
Mean discharge	193	191	216	221
Max daily mean	294	225	307	240
Max hourly mean	324		324	
Min daily mean	96	151	159	176
Min hourly mean	59		139	

For the present calculations no attempt was made to incorporate the actual values of discharges during the period of integration in view of the minor contribution from these sources to the total water circulation. Instead, an estimate of the average flow through Lake Ontario was arrived at in the following manner. Based on discharge measurements of the Trent River, the Moira River, etc., the total discharge from the Bay of Quinte into Lake Ontario may be estimated at 10 units. It seems reasonable to assume that this water flows more or less directly around Amherst Island into the St. Lawrence. Much of the water from the drainage area to the east of the lake does not affect the overall circulation of Lake Ontario either.

Thus the average St. Lawrence discharge is taken to be somewhat less than the average observed discharge, say, 200 units. Similarly, the average Niagara discharge may be slightly increased to 200 units in order to account for the contributions from the southern drainage basin. Thus the inflow and outflow balance each other for the duration of the experiment.

2. FORMULATION OF NUMERICAL MODEL

A detailed description of the numerical model has been presented elsewhere (Simons, 1971b) and the following is only a brief outline of the computational aspects of the experiment. The lake is assumed to be homogeneous, incompressible, and hydrostatic. The equilibrium depth is h, the elevation of the free surface above the undisturbed level is denoted by ζ, and u and v are the components of the horizontal velocity along the x- and y-axes of a right-handed coordinate system with the z-axis pointing upward. The volume transport components are defined

$$U \equiv \int_{-h}^{\zeta} u\,dz \qquad V \equiv \int_{-h}^{\zeta} v\,dz \tag{2}$$

The nonlinear inertial terms are discarded from the equations of motion on the basis of an evaluation of their effects in earlier studies. The vertically-integrated equations of

motion and the continuity equation then appear in the following form,

$$\frac{\partial U}{\partial t} = -gh\frac{\partial \zeta}{\partial x} + fV + \frac{\tau_{sx}}{\rho} - BU + A\nabla^2 U \qquad (3)$$

$$\frac{\partial V}{\partial t} = -gh\frac{\partial \zeta}{\partial y} - fU + \frac{\tau_{sy}}{\rho} - BV + A\nabla^2 V \qquad (4)$$

$$\frac{\partial \zeta}{\partial t} = -\frac{\partial U}{\partial x} - \frac{\partial V}{\partial y} \qquad (5)$$

where t is time, g is the acceleration of the earth's gravity field, f is the Coriolis parameter taken to be $10^{-4}sec^{-1}$, ρ is the density of water, τ_{sx} and τ_{sy} are the wind stress components at the surface, A is a coefficient of sub-grid-scale diffusion of momentum, and B is a coefficient of bottom friction. Based on earlier computations the diffusion coefficient is estimated at $A = 10^6 cm^2/sec$ for the present computational grid, and the bottom stress is approximated by $B = b/h^2$ where b is a constant of the order of 100 cm^2/sec when h is expressed in cm.

The equations are integrated by finite differences in time and space. Centered space differences are used in the interior of the lake and one-sided differences at the shore. A two-lattice type numerical grid is employed such that both components of the velocity are specified at a streampoint and each point at the centre of a square formed by four such points is an elevation point. The computational grid is shown in Figure 1 where the velocities are specified in the corners and the surface elevations at the centre of

each square. The depths of the lake are given in the streampoints and in the boundary streampoints the depths and both components of the water transport vector are set equal to zero. Where the diagonal boundary segments pass through elevation points (half squares) the surface elevation is computed from the continuity equation by forward space differences. All finite differences are evaluated along coordinates rotated over 45 degrees with respect to the meridians and the parallels. The grid mesh is 5.08 km, hence the interval over which centered differences are computed is about 7 km. Only the Laplacians in the diffusion terms are evaluated by finite differences along the meridians and the parallels.

For the time integration of the basic wave-related terms centered time-differences are used. Thus the surface elevation is staggered in time with respect to the velocities. The Coriolis term is treated by time interpolation and the bottom stress and the horizontal diffusion are evaluated at the previous time level. The time step at which each of the variables is computed is 100 sec, which is the time interval over which centered time differences are evaluated. Since the wind stresses are available only at one-hour intervals a simple linear interpolation is used to obtain the wind input for each time step.

The two-lattice type grid is rather sensitive to grid dispersion, i.e., the decoupling of solutions on the individual lattices. In particular it is necessary to distribute the river discharges equally over both lattices. The grid dispersion of the surface was computed at regular time intervals and was found to stay within acceptable limits. Furthermore, the river discharges were initially set equal to zero and in the course of one day increased to the above mentioned values in order to prevent the formation of a large surge.

3. RESULTS OF FLOW COMPUTATIONS

Before proceeding to a description of the daily flow patterns for the present experiment we may consider the circulation of Lake Ontario in the absence of wind forcing. In that case the water movements are the result of the river discharges discussed in the first section. Since the model starts from a state of rest it takes some time for the circulation to adjust to a quasi-steady pattern. After a few days, however, the changes become minor and after about 5 days the model appears to have reached a steady state. Figures 2.1 and 2.2 show the volume transports for this case after 2 days and 10 days, respectively. Notice that the scale of the transport vectors has been reduced in the

second figure. It is clear that the circulation tends to be concentrated in the northern half of the lake and a weak return flow seems to establish itself in the deeper parts of the lake. It should be noted though, that this result depends on the horizontal eddy diffusivity and the bottom stress and some uncertainty remains concerning the best formulation of these parameters.

For comparison with this steady flow we will next present the average circulation for the duration of the present experiment as an example of the long-term mean lake circulation under average wind conditions. The mean flow pattern was obtained by averaging the hourly model output for April 20 through May 14, 1971. The river discharges are included in all computations. Figure 3 shows the volume transports for this mean circulation together with the average wind stress for this period (in the upper left-hand corner of the map). The magnitude of the wind stress turns out to be .16 cm^2/sec^2 and the stress vector is indeed in the general direction of the long-term average for Lake Ontario. As expected for such wind forcing, the circulation exists of westward currents along the shores and return flow in the deeper portions of the lake.

Turning now to a detailed discussion of the present experiment we will first consider the energy of the lake in relation to the wind stress at the surface. The energy supplied by the wind to the lake can be partitioned in potential and kinetic energy. For the homogeneous lake the kinetic energy averaged over the whole lake volume is

$$KE = \frac{1}{2} \int_S \frac{U^2+V^2}{h} \, dxdy \Big/ \int_S h \, dxdy \qquad (6)$$

where S is the surface area of the lake. In this case the potential energy is determined completely by the surface elevation and it may be written in the same units as follows

$$PE = \frac{1}{2} \int_S g\zeta^2 \, dxdy \Big/ \int_S h \, dxdy \qquad (7)$$

It may be noted that in the absence of external and frictional forces the sum of these two energy quantities is conserved by the model.

The surface stress components and the lake energy parameters for April 20 to May 14, 1971 are shown in Figures 4.1 and 4.2. The first two graphs from the top represent the eastward and the northward components of the surface stress computed from the wind records according to equation (1). These stress components may be related directly to the energy of the wind at the surface of the lake. The two bottom graphs picture the kinetic and the potential energy of the lake corresponding to the solutions obtained from the model.

All units are cm^2/sec^2. The kinetic energy shows the tremendous impact of the sustained storm of April 23-25, 1971, and it appears reasonable to venture that this episode annihilated most of the previously existing water circulations. Therefore, the initial conditions of no motion imposed on the model will probably not introduce serious errors in the subsequent solutions. The potential energy is much smaller than the kinetic energy but the scale of the bottom graph of Figure 4 has been enlarged to visualize its quasi-periodic behavior. The five-hour period of longitudinal oscillation of Lake Ontario shows up after every episode of strong winds in the form of pronounced peaks of potential energy at $2\frac{1}{2}$ hour intervals. Much of this can probably be ascribed to the uniform wind stress which will generally result in a more oscillatory solution than a storm moving across the lake as shown, for example, by Rao (1967).

Figures 5.1 through 5.9 show daily circulation patterns for the first ten days of the experiment (starting with the second day) and Figures 5.10 to 5.12 present the circulation at five day intervals for the last 15 days. All maps apply to the end of the day indicated in the upper left-hand corner, and the vectors at the top of the maps represent the wind stress history preceding the map time and starting

with the previous map. Thus in the first nine maps the stresses are pictured at hourly intervals, in the last three maps at six-hourly intervals. The vectors within the lake boundaries again represent the volume transports defined earlier, that is, the vertically integrated velocities. Note that the scales of the transport vectors differ from one map to the next. Although this improves the visual display of the individual maps it does not immediately expose the large variations in velocities and it is worthwhile to point out that the average velocities on April 25 are about five times greater than after the passage of this storm. The general pattern of the flow is such that the boundary currents are in the direction of the wind with return flow occurring in the deeper parts of the lake. Since the bottom falls off rapidly at the southern shore the boundary currents are locally very narrow or non-existing.

During the first week of the experiment the wind is blowing nearly continuously from the northwest. This results in a well-defined large clockwise circulation cell covering most of the lake. The velocities associated with this pattern reach a maximum on April 25, after which the lake-wide cell tends to break up in a number of smaller vortices. In particular, a strong anti-clockwise circulation cell establishes itself in the southeastern portion of the lake, which can be traced back to the southern boundary current in the

earlier maps. Under influence of the complete wind reversal of April 28 this anti-clockwise cell is able to extend itself into the central lake basin and only in the western end of the lake a clockwise circulation remains. After the wind returns to westerly on April 29, a much less organized circulation associated with relatively low velocities is left. The general character of this cycle of events can be observed also on subsequent days. Thus the northwesterly winds of May 3 and May 4 result in the lake-wide clockwise circulation reminiscent of the first days of the experiment. Again after the wind reversal of May 8 a large number of smaller-scale vortices with relatively low velocities remain. The last day of the experiment sees the return of the large clockwise circulation cell covering the western and central basin and the small anti-clockwise cell in the south-eastern portion of the lake, which apparently are the most common features of the circulation of Lake Ontario. Indeed these cells constitute the primary components of the average circulation for this period shown in Figure 3.

4. APPLICATIONS OF COMPUTED FLOW

The water circulations computed by the hydrodynamic model bear important implications concerning the advective transport of dissolved or suspended matter in the lake. The

transport of matter in the lake can be visualized as the combined effect of advection and diffusion. The advective transport of material is ascribed to the large-scale organized water currents which are computed by the model. The second process is the flux of mass resulting from quasi-random motions of scales smaller than the numerical grid. This sub-grid-scale diffusion is assumed to be proportional to the gradient of the concentration of matter multiplied by an eddy diffusivity A. The general conservation equation describing the behavior of a given water quality parameter of concentration C per unit volume in a vertically-homogeneous lake may be written

$$\frac{\partial C}{\partial t} + \nabla . \left[\mathbf{V}C - hA\nabla C \right] = \frac{1}{h}(S_s + S_b) + S_i \qquad (8)$$

where $\mathbf{V}$ is the water transport vector, ∇ is the gradient operator, S_s and S_b are the sources of material at the free water surface and the bottom per unit area, and S_i represents the internal generation or decay of substance per unit volume.

As an example of the application of this equation we will here discuss the advection and diffusion of a conservative parameter (zero sources and sinks) introduced in Lake Ontario via the Niagara River. Since this material enters through the lateral walls of the model, the source

terms on the right of the advection-diffusion equation are set equal to zero and the concentration of pollutant is specified at the mouth of the Niagara River. This concentration is set equal to 10 units and is maintained at that value for the duration of the experiment. We now consider four cases corresponding to two advective flow patterns and two diffusion coefficients in order to demonstrate the effects of these individual processes. The first advective flow is the steady state circulation without wind shown in Figure 2, the second current pattern is based on the wind-induced circulations computed for April 20 to May 14, 1971 and shown in Figures 3 and 5. For the turbulent diffusion parameter we may have recourse to empirical investigations of diffusion characteristics by dye-release experiments in oceans (Okubo, 1971) and lakes (Murthy, 1970). Such studies derive an apparent diffusivity versus the scale of diffusion, which for intermediate scales of the order of 1 to 10 kilometers ranges between 10^4 and 10^5 cm^2/sec. Assuming that these are the upper and lower limits of the eddy diffusivity A we will compare the effects of these two values.

Figures 6.1 and 6.2 show the computed concentrations after one half year if the pollutant is advected by the river-related circulation of Figure 2. The first figure is for the lower value of the eddy diffusivity, the second figure presents

the result of using the upper value of the coefficient mentioned earlier. From a glance at these results it will be apparent that in the first case the diffusion is negligible by comparison with the advection since the pollutant clearly follows the path of the water mass as it flows from the Niagara to the east. In the second case, however, the effects of diffusion and advection become comparable in magnitude and the pollutant tends to disperse more symmetrically with respect to the river mouth. It would follow then that the results for this case are largely governed by the values of the diffusivity.

Figures 7.1 and 7.2 show the results of similar calculations if the advective flow is replaced by the transports computed for April 20 - May 14, 1971. Since the period of integration of the dispersion problem is much larger than the length of time of the hydrodynamic experiment, we assume that the circulation of the lake is periodic with a period of 25 days such that we can re-cycle the computed circulation for use in the advective terms of the dispersion equation. Such computations have of course no predictive value but still should give a good indication of the long term effects of the highly variable currents induced by the wind. The computations were also repeated after substituting the averaged flow of Figure 3 for the full period of integration and the results turned out very

similar. The results shown in Figures 7.1 and 7.2 are again for one half year of integration and for the lower and the higher values of the diffusivity, respectively. The most pronounced aspects of these calculations are that the effects of the wind-induced circulation completely obscure the hydraulic effects and that the dissolved matter tends to be carried to the north-western shore rather than along the southern shore of the lake. Considering that the direction of the present average wind is fairly typical for Lake Ontario we may attach some significance to this solution in spite of the simplifications involved in the model. At any rate, the solutions for the case including wind show that the advection by the wind-induced currents is most significant even if the higher value of the diffusivity is used. Consequently it appears necessary to compute the large scale water circulations for a study of the dispersion of pollutants in a lake.

A second example of the use of water transports computed by the hydrodynamical model concerns the movements of particulate matter across a vertical crosssection of the lake. Again this transport consists of two contributions. The advective transport by the large-scale currents is equal to the product of the vertically integrated water transport normal to the vertical interface, V_n, and the concentration

per unit volume,C. Thus the advective flux per unit of horizontal distance along the vertical crosssection is

$$F_{adv} = V_n.C \qquad (9)$$

The diffusive flux contributed by the small-scale turbulent water motions is proportional to the gradient of concentration normal to the vertical crosssection. Thus if n indicates this direction, then the flux per unit of horizontal width is

$$F_{dif} = -h.A.\frac{\partial C}{\partial n} \qquad (10)$$

where the minus sign indicates that the flux is in the direction of decreasing concentration.

It is seen from the above that the advective flux is determined essentially by a correlation of concentration of material on the one hand and the volume transport of water normal to the crosssection on the other. The latter is derived immediately from the output of the hydrodynamic model. As an example we may consider the water transport through a vertical crosssection of Lake Ontario along the international border indicated by the dashed line of Figure 1. Figures 8a and 8b show this transport (counted positive from the U.S. side to the Canadian side) for each day of the experiment discussed in the previous section as a function of the distance along the border from the Niagara to the St. Lawrence. It is seen that large day-to-day variations occur in the distribution of the transports along the border depending on the wind conditions.

REFERENCES

OKUBO, A., 1971: Oceanic Diffusion Diagrams. Deep Sea Research, 18, 789-802

MURTHY, C.R., 1970: An Experimental Study of Horizontal Diffusion in Lake Ontario. Proc. 13th Conf. Great Lakes Res., 477-489

RAO, D.B., 1967: Response of a lake to a Time-Dependent Wind Stress. J. Geophys. Res., 72, 1697-1708

SIMONS, T.J., 1971a: Development of Numerical Models of Lake Ontario. Proc. 14th Conf. Great Lakes Res., 654-669

SIMONS, T.J. 1971b: Development of three-dimensional numerical models of the Great Lakes, Canada Centre for Inland Waters, Scientific Report, 85 pp.

TAYLOR, W.B., 1971: Summary of the 1971 Lake Ontario Meteorological Buoy Stations. Canada Centre for Inland Waters, Technical Report, 11 pp.

WATER SURVEY OF CANADA, 1970: Surface Water Data, Ontario, Water Year 1967. Inland Waters Branch, Dept. of EMR, Ottawa.

FIGURES

Figure 1. Numerical grid of streampoints. Surface elevations are defined at the centre of each square. Black circles indicate locations of meteorological buoys.

Figures 2.1-2 Volume transports for hydraulic flow of Lake Ontario 2 days and 10 days, respectively, after start of model.

Figure 3. Volume transports for average flow computed for April 20 to May 14, 1971. Average wind stress shown in upper left hand corner.

Figures 4.1-2 Eastward and northward components of the wind stress for April 20 to May 14, 1971, and kinetic and potential energy of Lake Ontario computed for this period.

Figures 5.1-12 Water transports in Lake Ontario for several days in April and May 1971 as computed by the model. Wind stress history at equal intervals between current and previous map indicated at the top of the map.

Figures 6.1-2 Concentration of conservative matter introduced via the Niagara River in Lake Ontario after one half year of computation. Advective flow corresponding to Figure 2, coefficient of eddy diffusion equal to 10^4 and 10^5 cm^2/sec, respectively.

Figures 7.1-2 Same as Figures 6.1-2 but advective flow of Figure 3.

Figures 8.1-2 Water transport from south to north across the international border in Lake Ontario per unit length along the border between the Niagara and the St. Lawrence, for each day from April 21 to May 14, 1971.

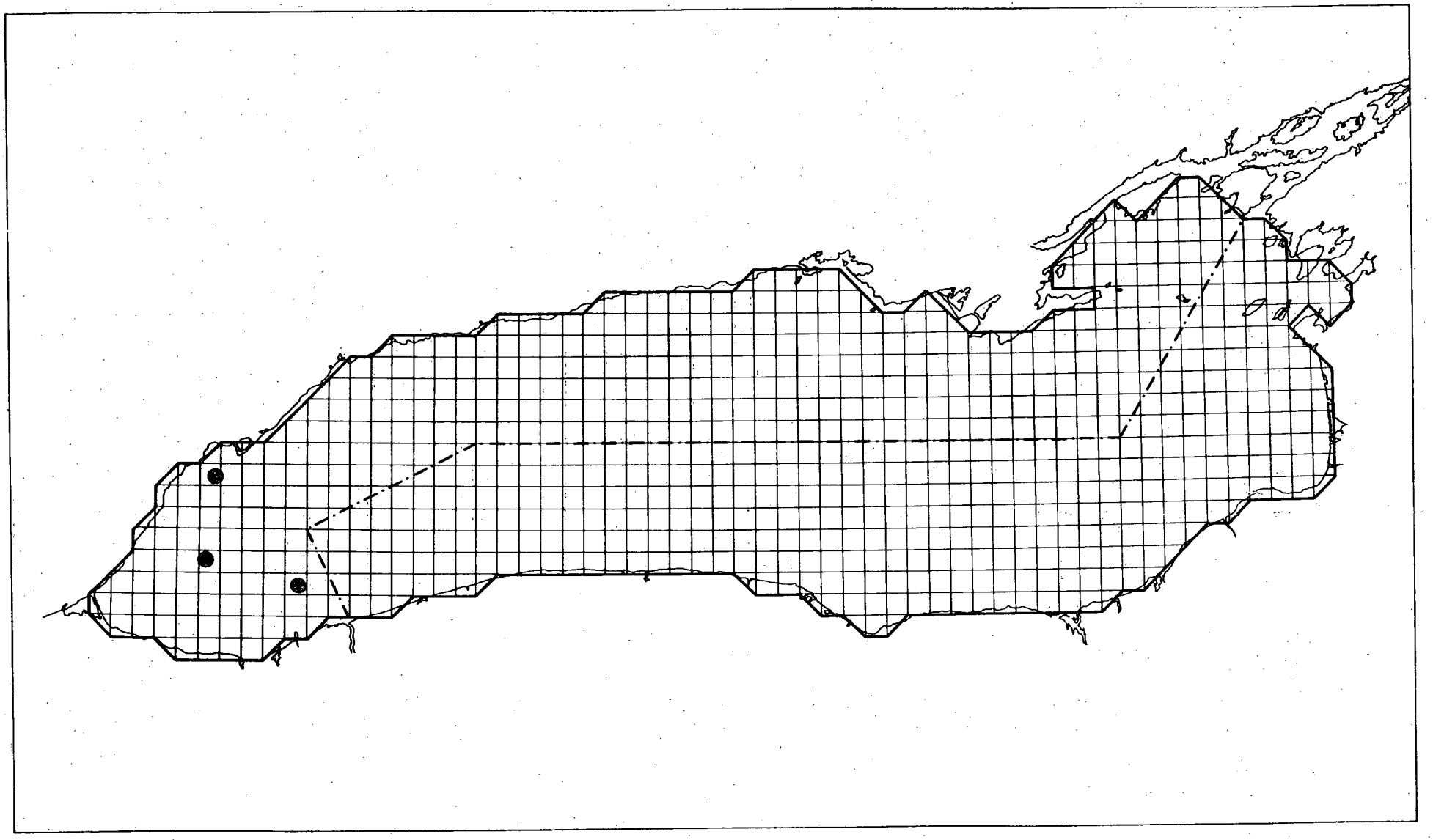

Figure 1.

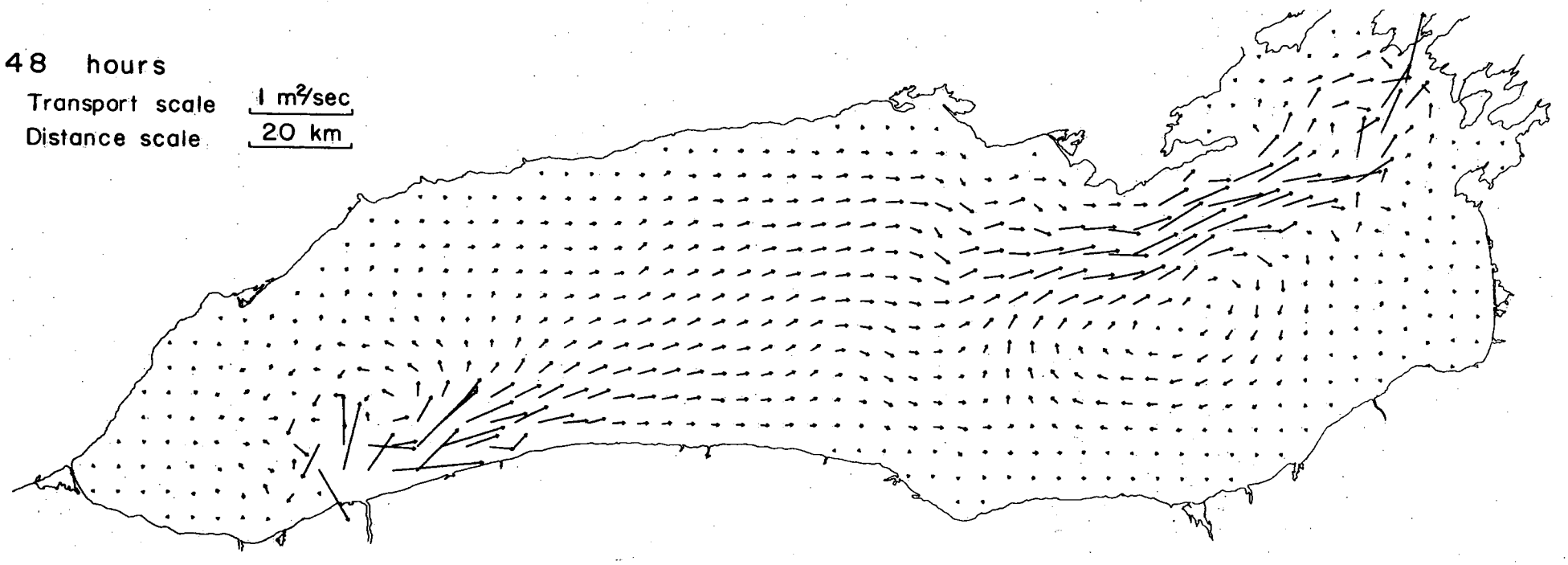

Figure 2.1

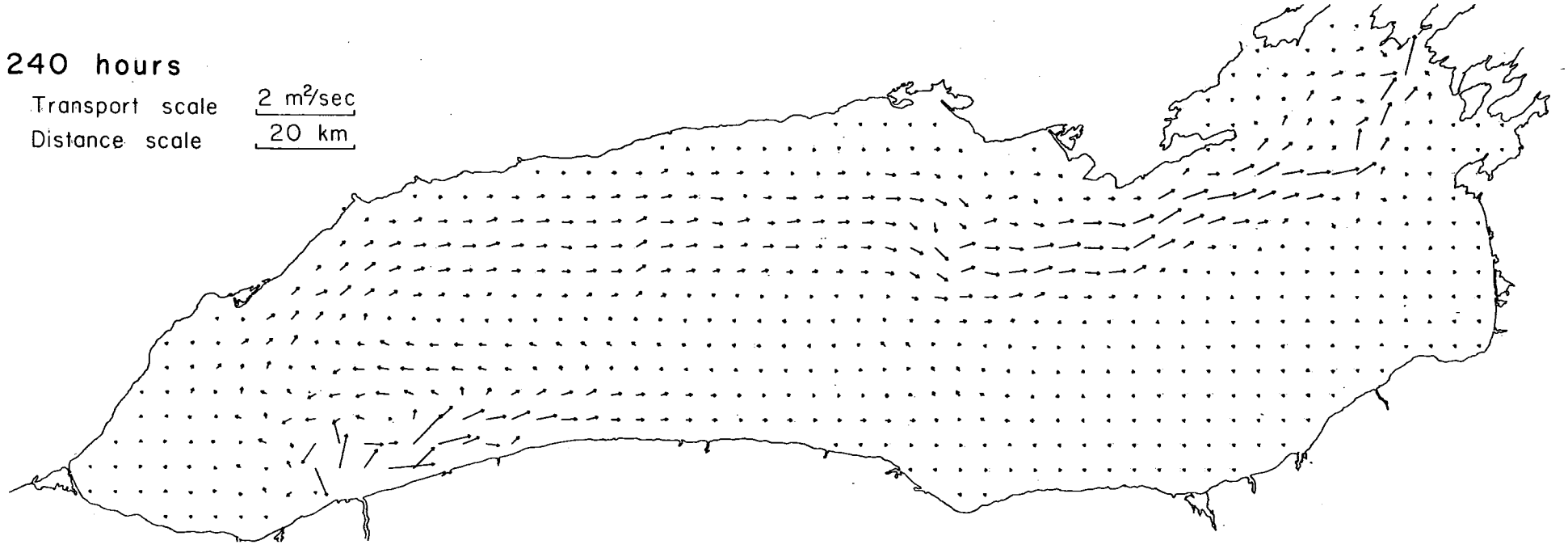

Figure 2.2

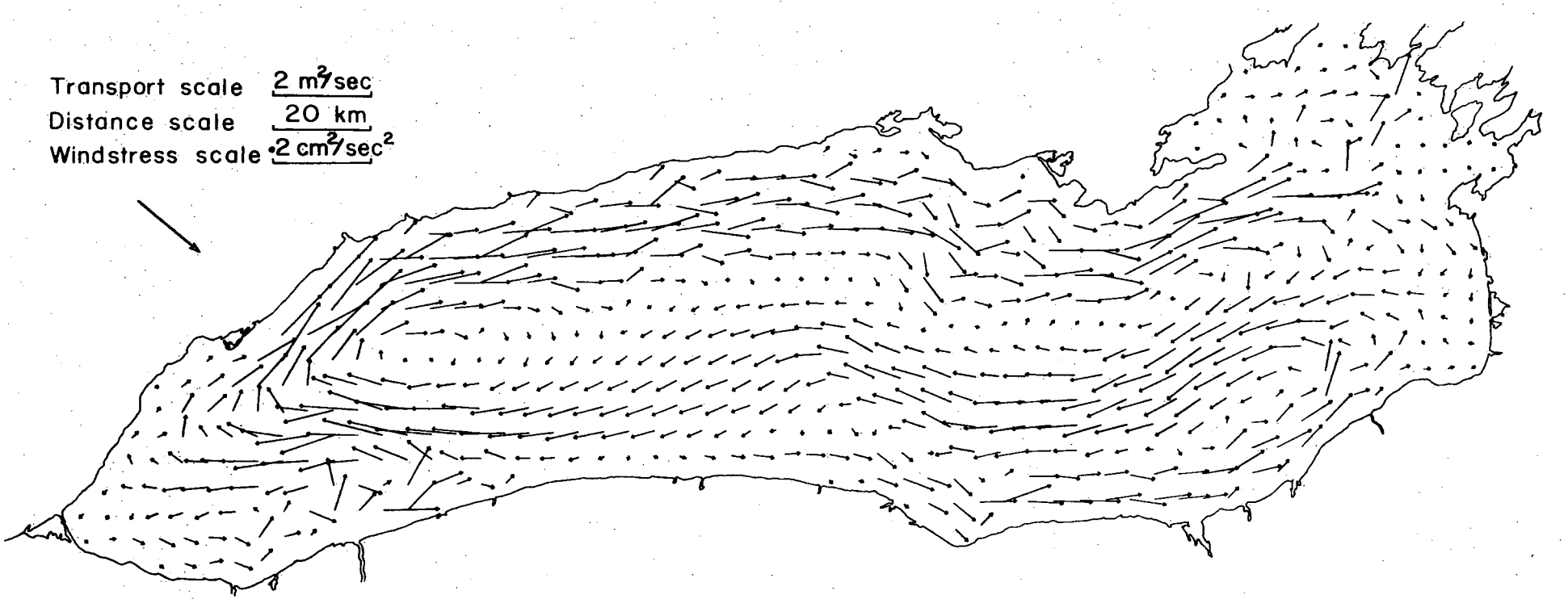
Transport scale 2 m²/sec
Distance scale 20 km
Windstress scale 2 cm²/sec²

Figure 3.

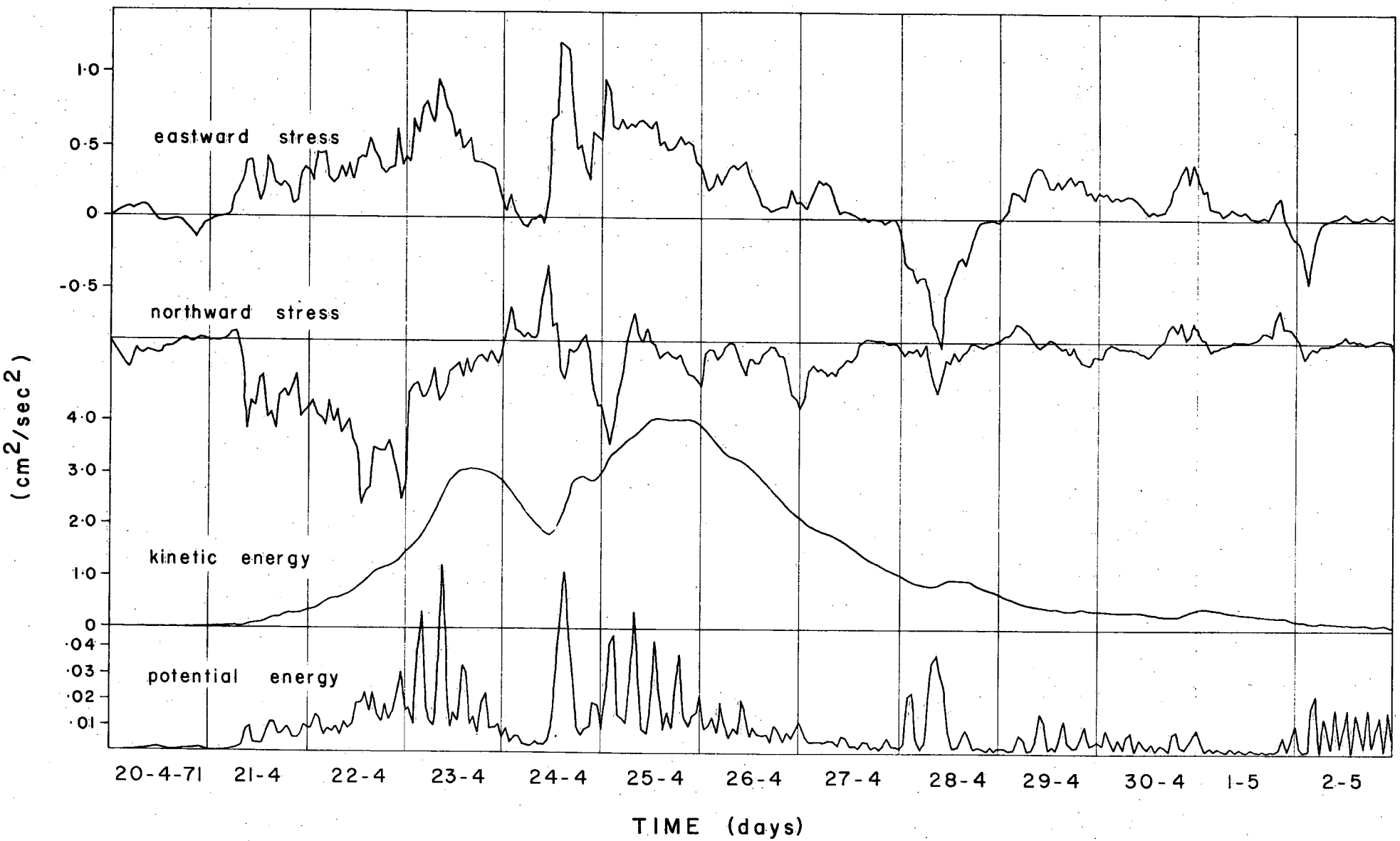
eastward stress
northward stress
kinetic energy
potential energy
1·0
0·5
0
-0·5
4·0
3·0
2·0
1·0
0
·04
·03
·02
·01
(cm²/sec²)
20-4-71
21-4
22-4
23-4
24-4
25-4
26-4
27-4
28-4
29-4
30-4
1-5
2-5
TIME (days)

Figure 4.1

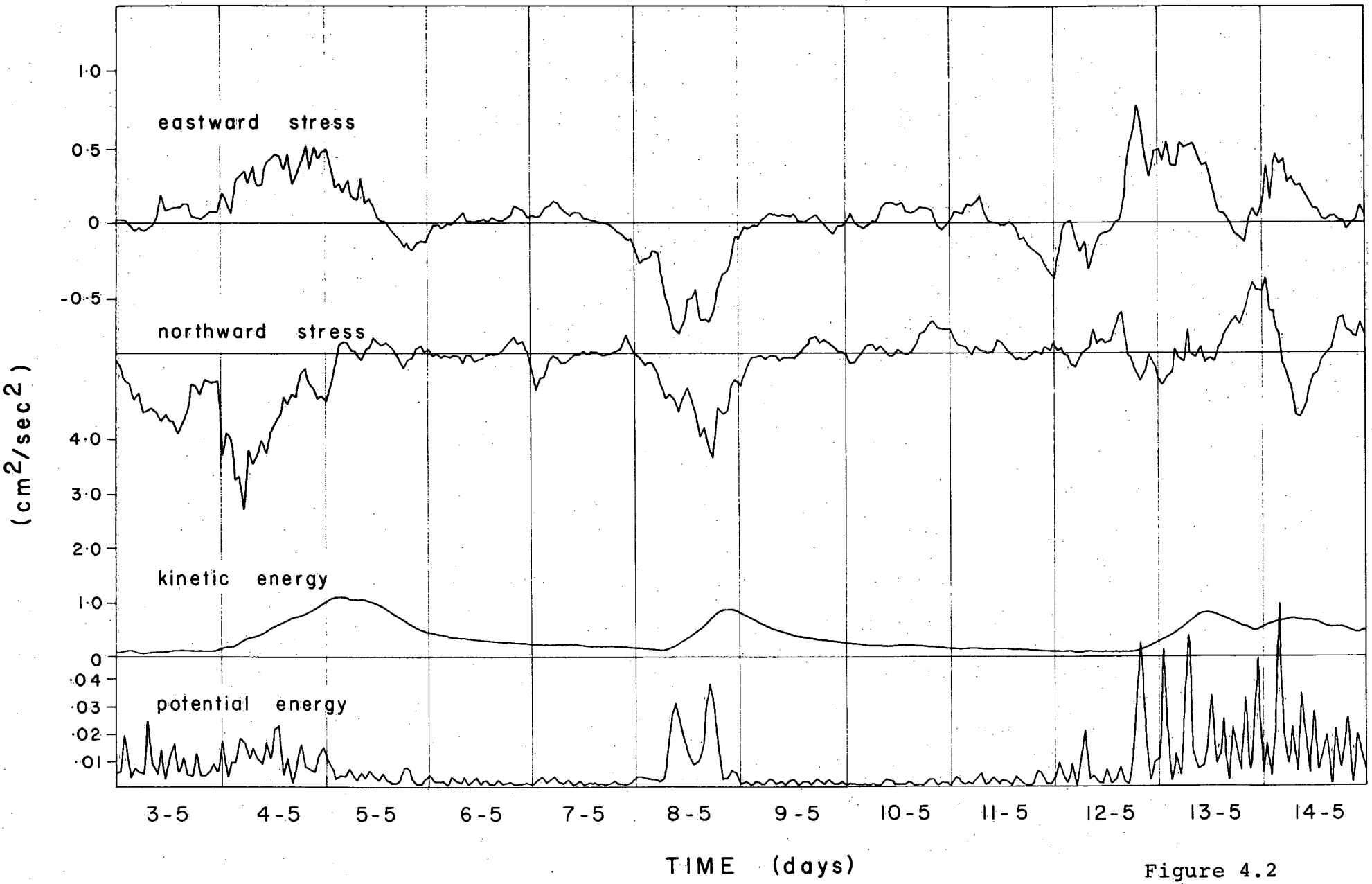
eastward stress
northward stress
kinetic energy
potential energy
1·0
0·5
0
-0·5
4·0
3·0
2·0
1·0
0
·04
·03
·02
·01
(cm²/sec²)
3-5
4-5
5-5
6-5
7-5
8-5
9-5
10-5
11-5
12-5
13-5
14-5
TIME (days)

Figure 4.2

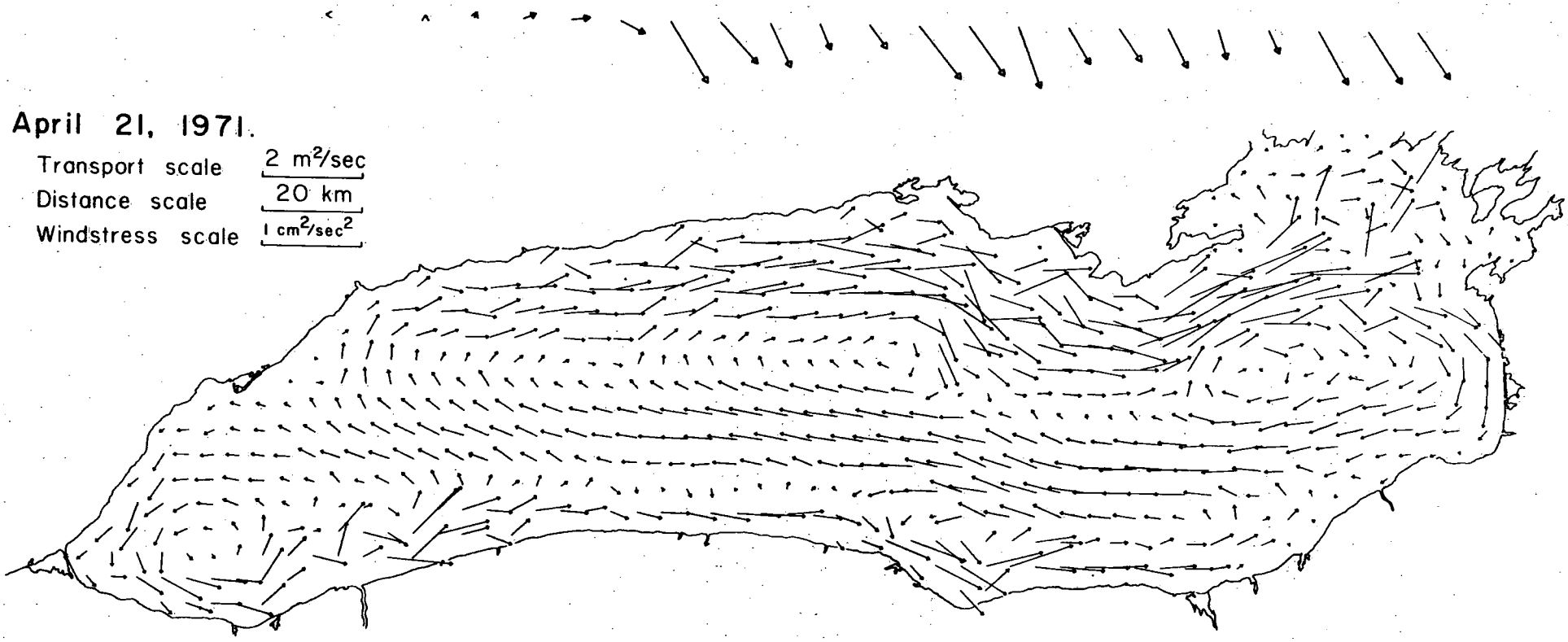
April 21, 1971.
Transport scale 2 m²/sec
Distance scale 20 km
Windstress scale 1 cm²/sec²

Figure 5.1

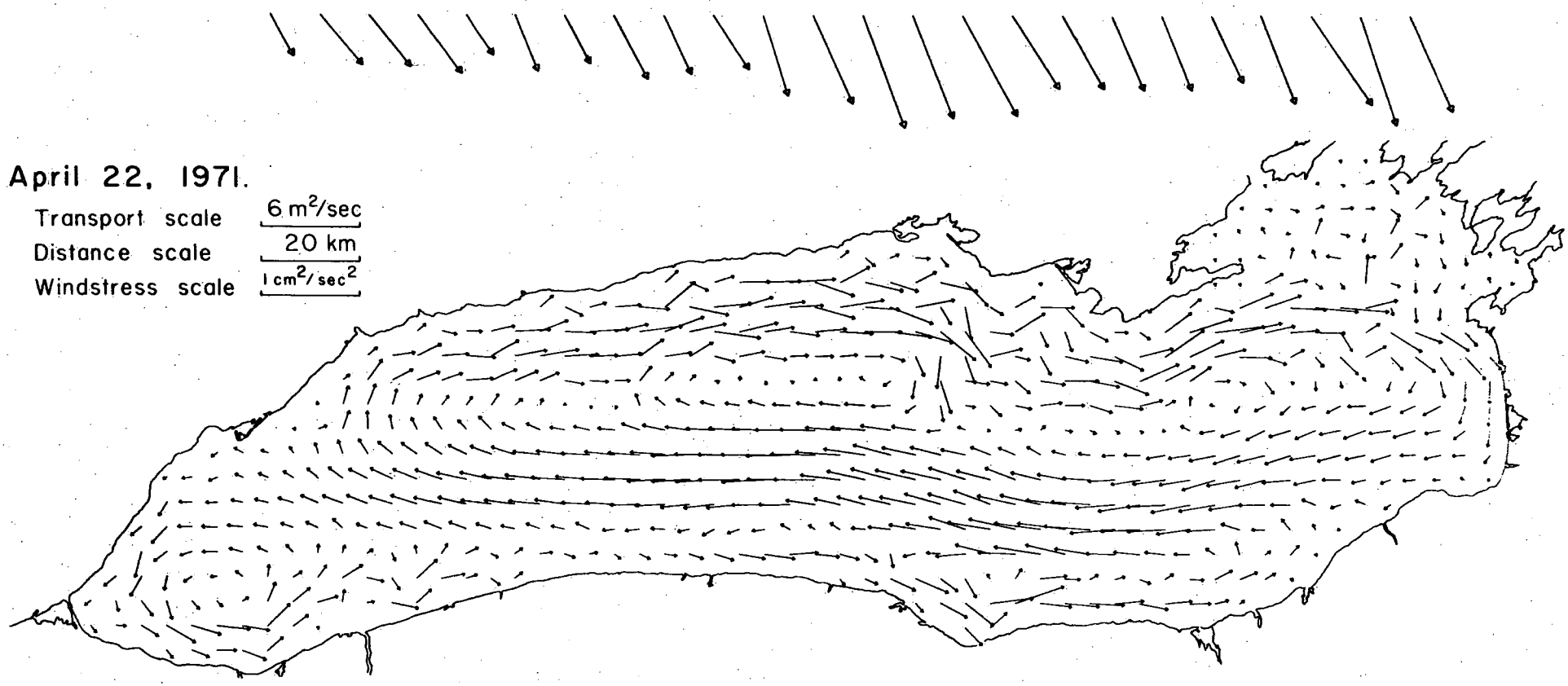
April 22, 1971.
Transport scale 6 m²/sec
Distance scale 20 km
Windstress scale 1 cm²/sec²

Figure 5.2

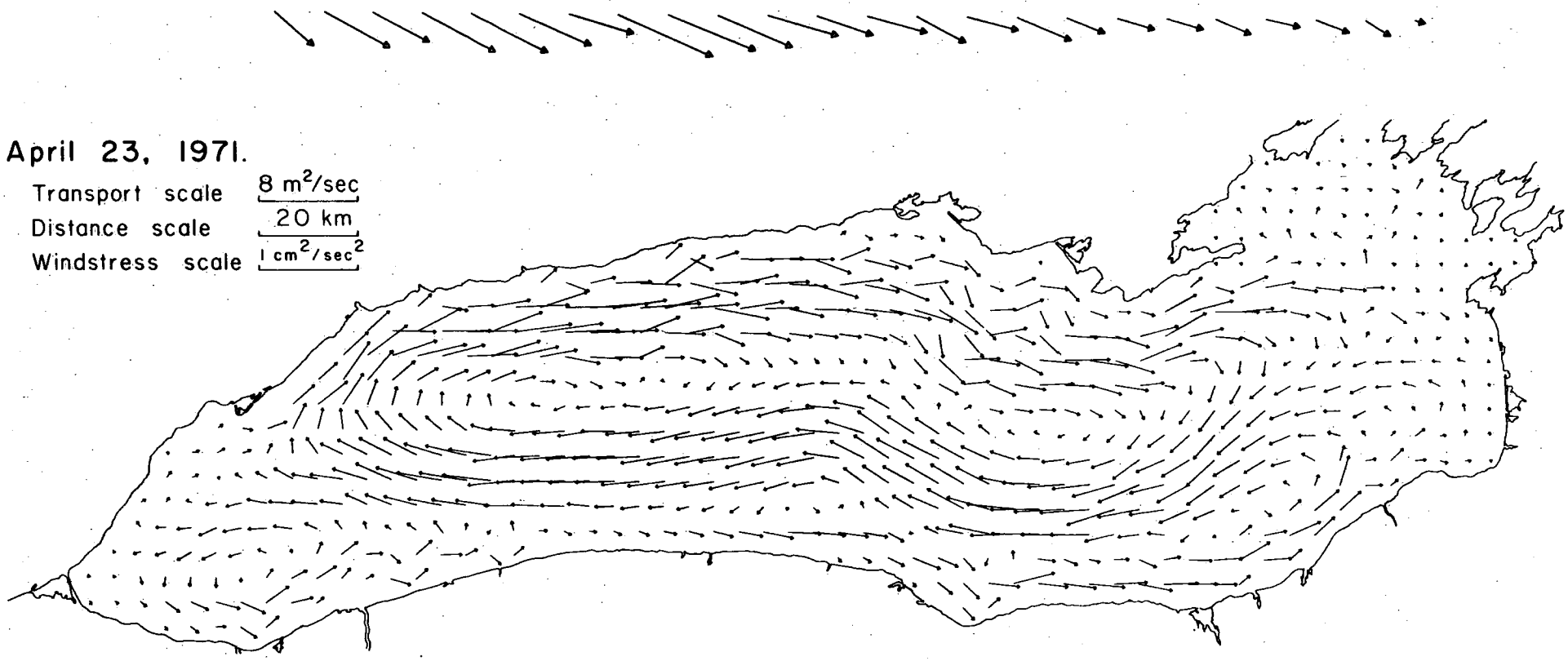
April 23, 1971.
Transport scale 8 m²/sec
Distance scale 20 km
Windstress scale 1 cm²/sec²

Figure 5.3

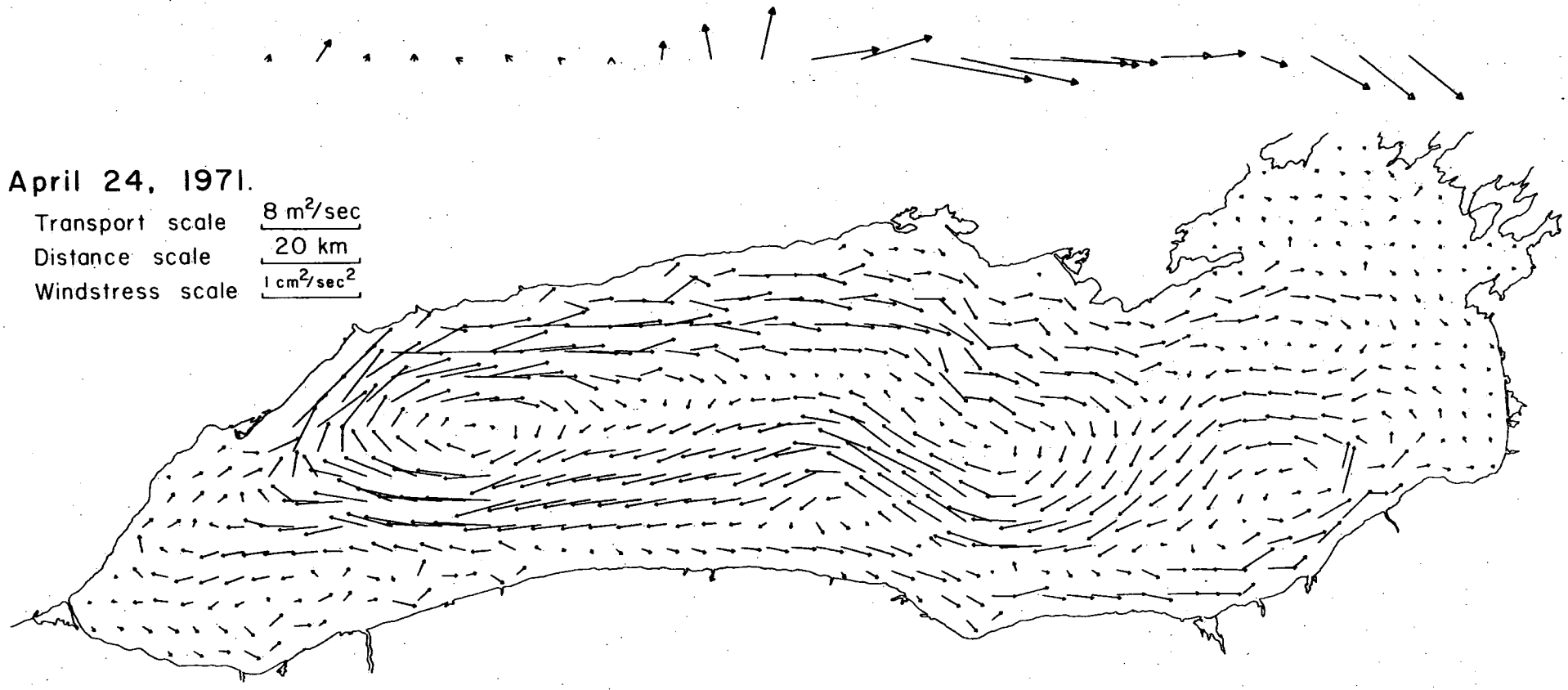
April 24, 1971.
Transport scale 8 m²/sec
Distance scale 20 km
Windstress scale 1 cm²/sec²

Figure 5.4

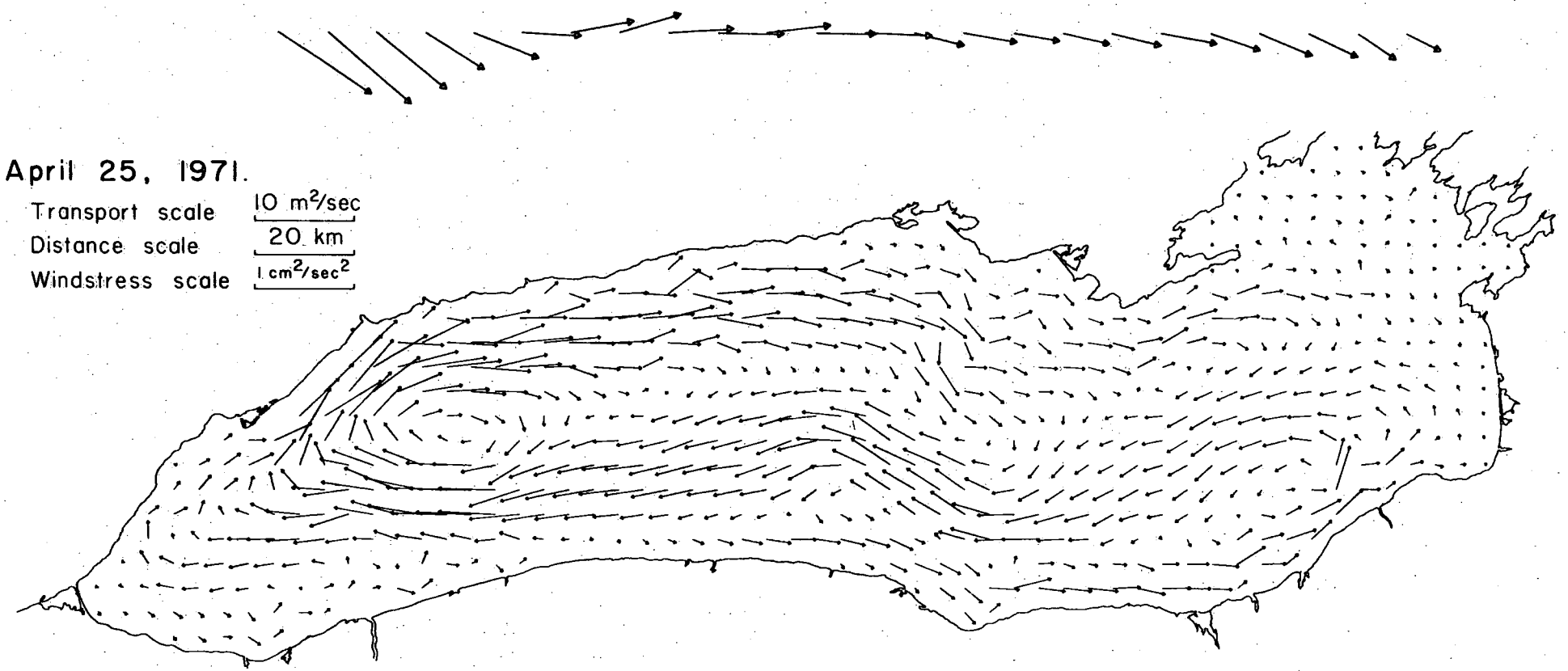
April 25, 1971.
Transport scale 10 m²/sec
Distance scale 20 km
Windstress scale 1 cm²/sec²

Figure 5.5

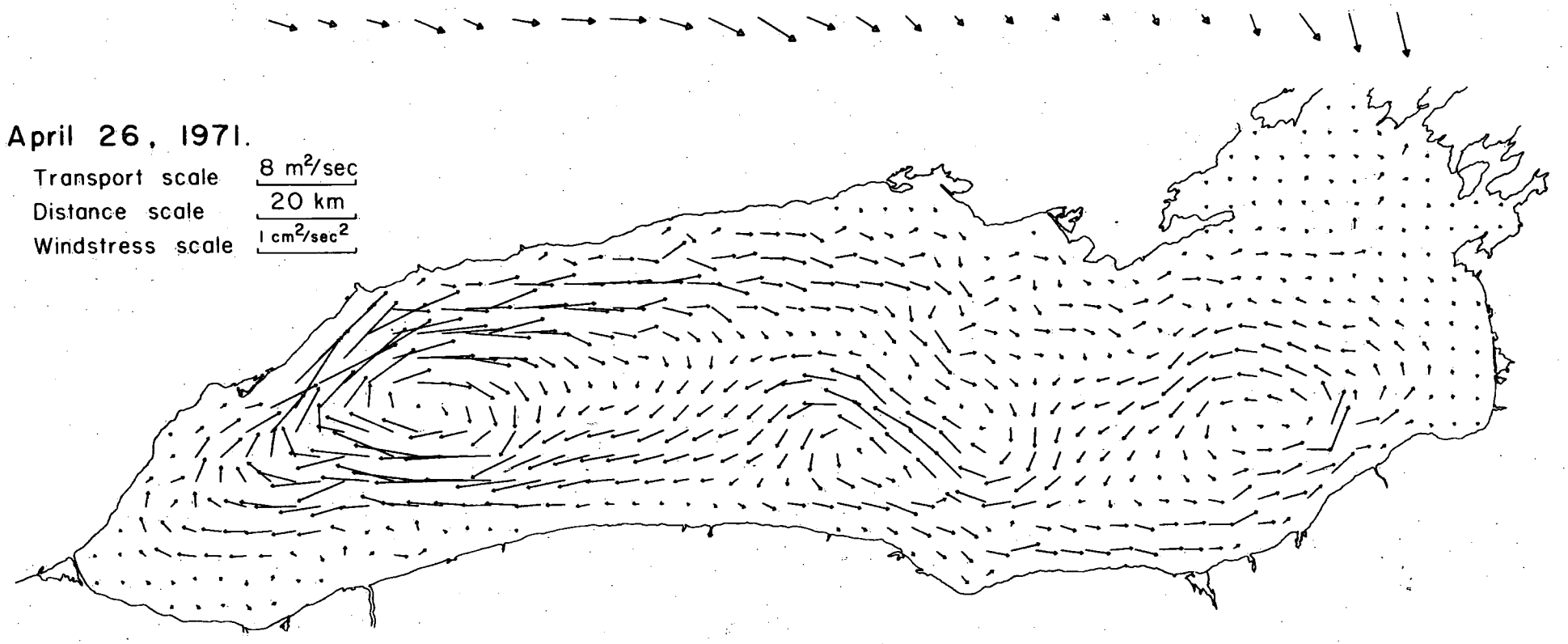
April 26, 1971.
Transport scale 8 m²/sec
Distance scale 20 km
Windstress scale 1 cm²/sec²

Figure 5.6

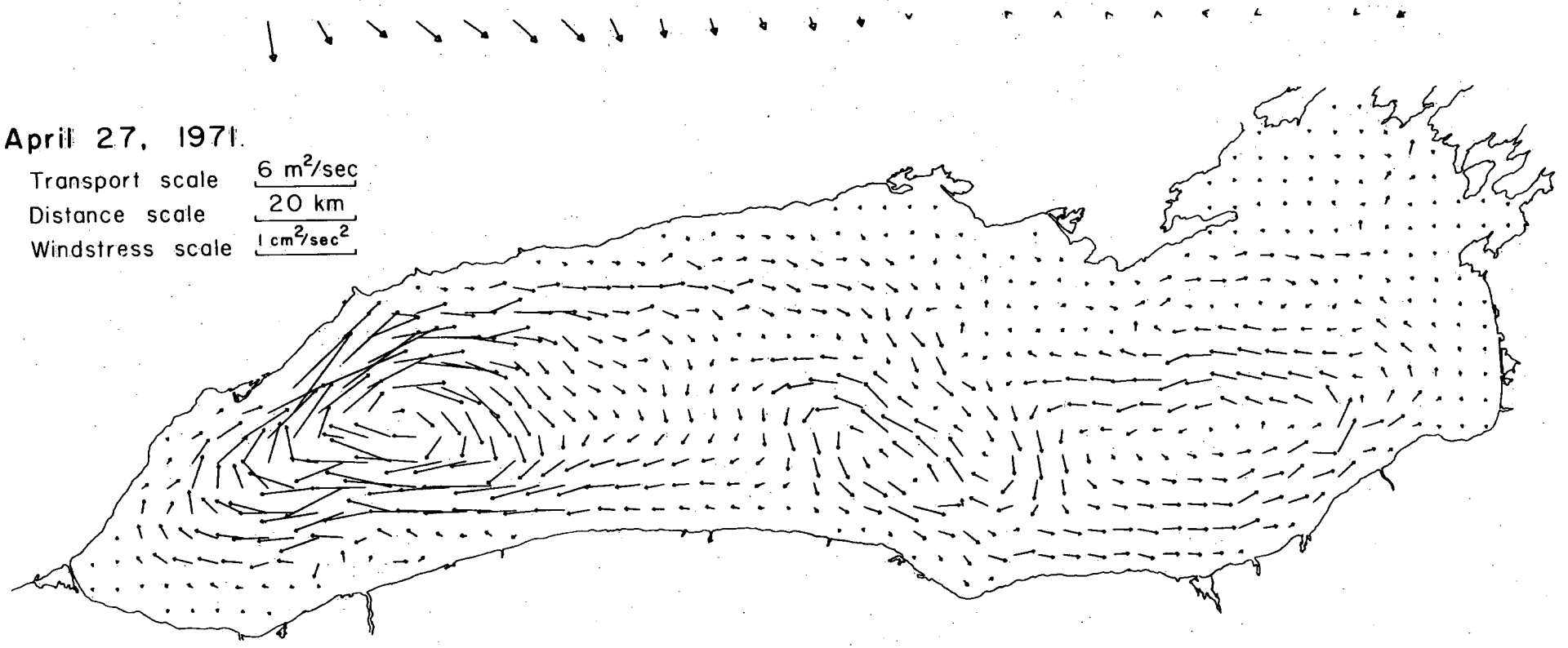
April 27, 1971
Transport scale 6 m²/sec
Distance scale 20 km
Windstress scale 1 cm²/sec²

Figure 5.7

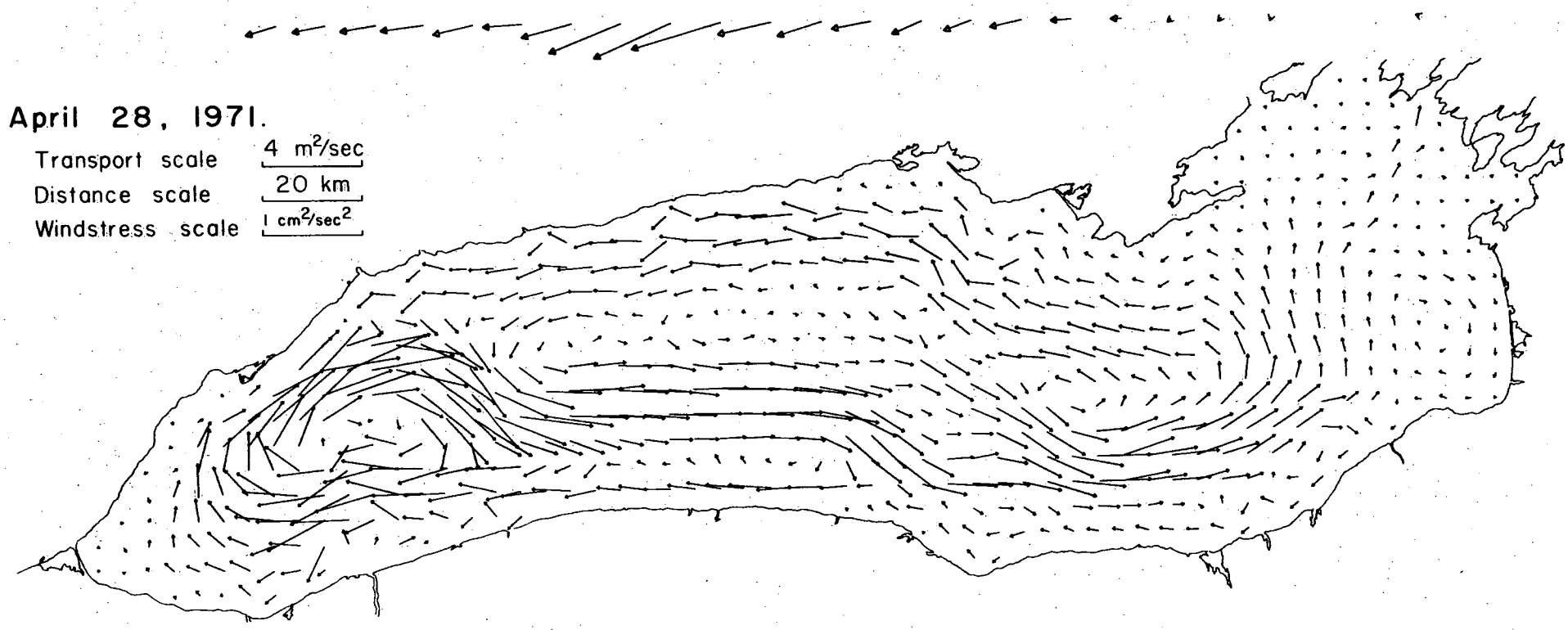
April 28, 1971.
Transport scale 4 m²/sec
Distance scale 20 km
Windstress scale 1 cm²/sec²

Figure 5.8

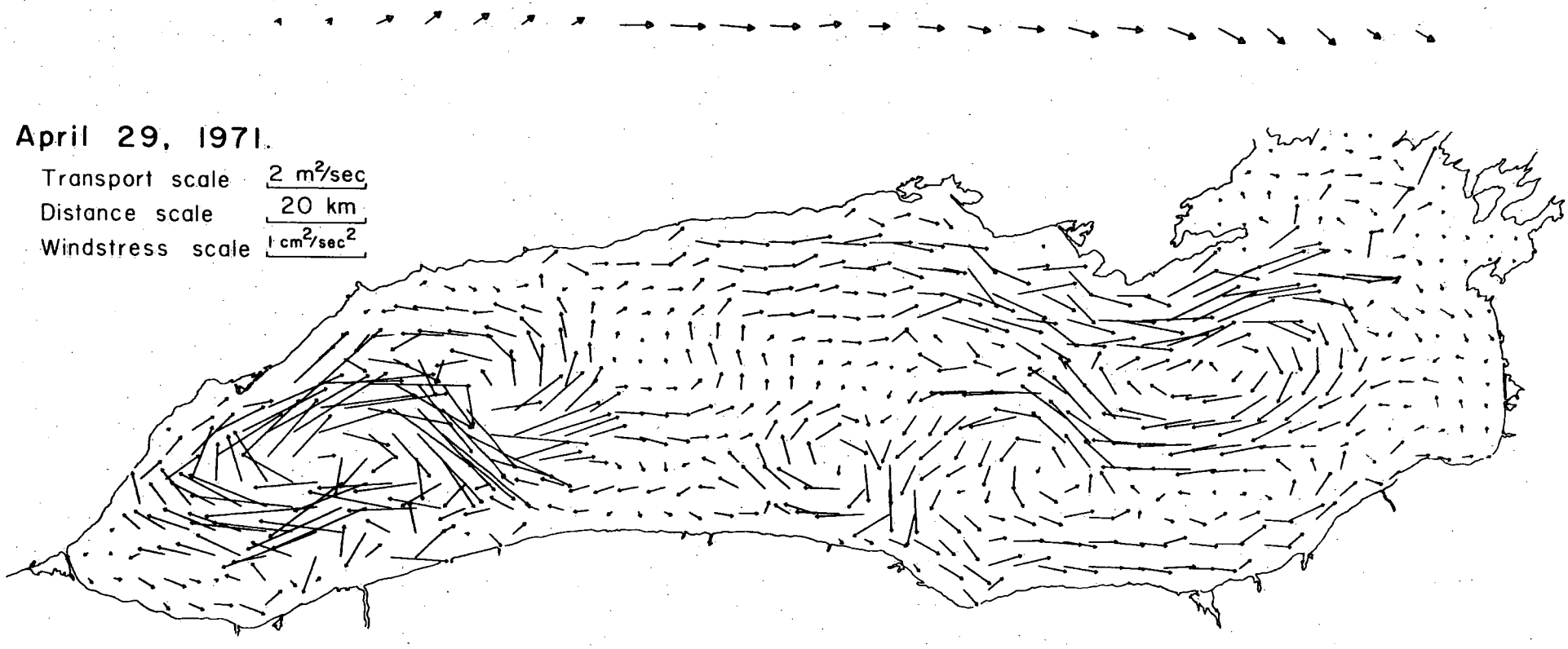
April 29, 1971.
Transport scale 2 m²/sec
Distance scale 20 km
Windstress scale 1 cm²/sec²

Figure 5.9

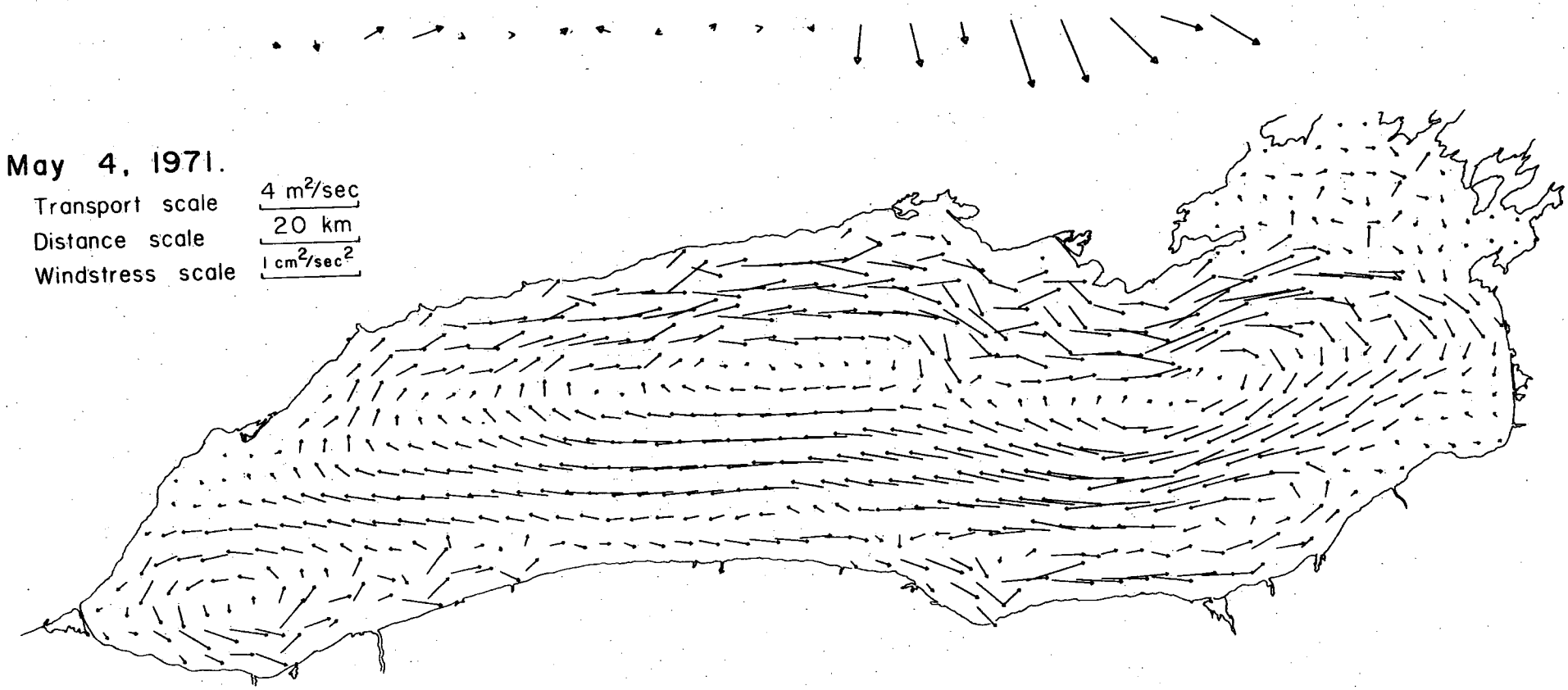
May 4, 1971.
Transport scale
4 m²/sec
Distance scale
20 km
Windstress scale
1 cm²/sec²

Figure 5.10

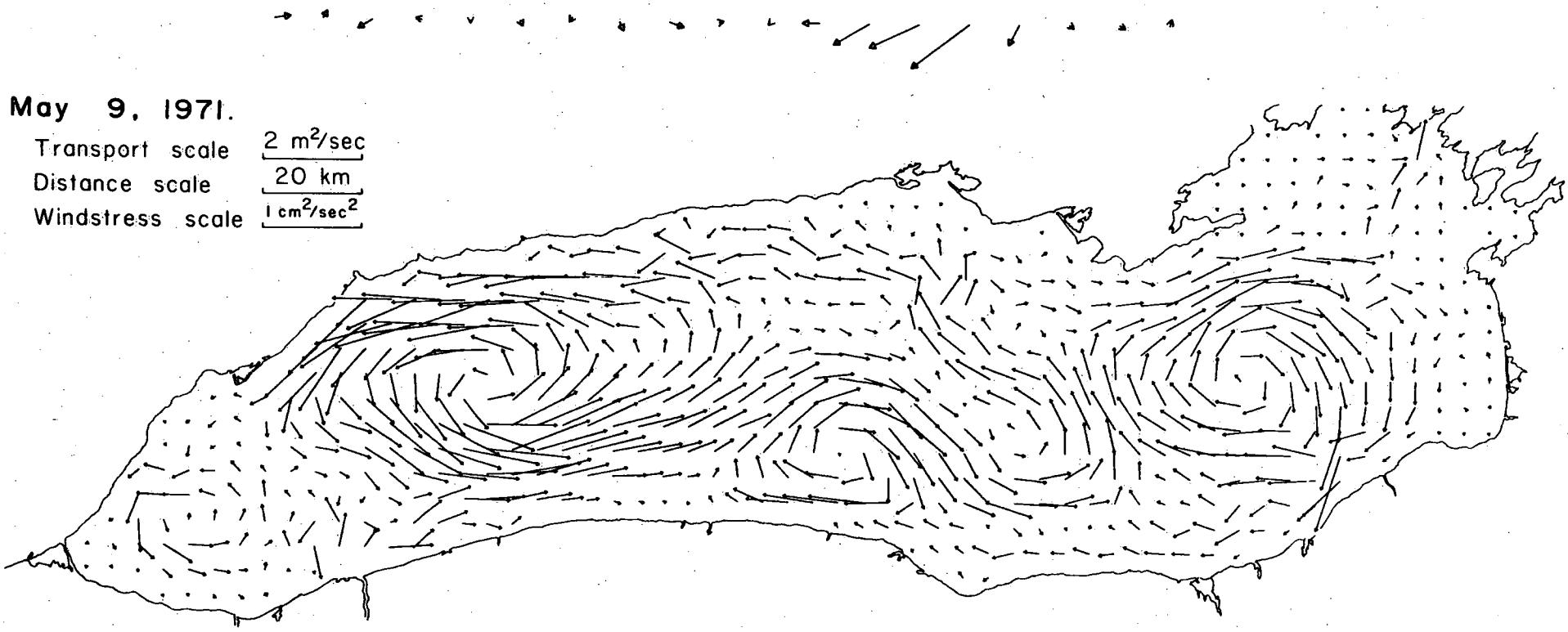
May 9, 1971.
Transport scale 2 m²/sec
Distance scale 20 km
Windstress scale 1 cm²/sec²

Figure 5.11

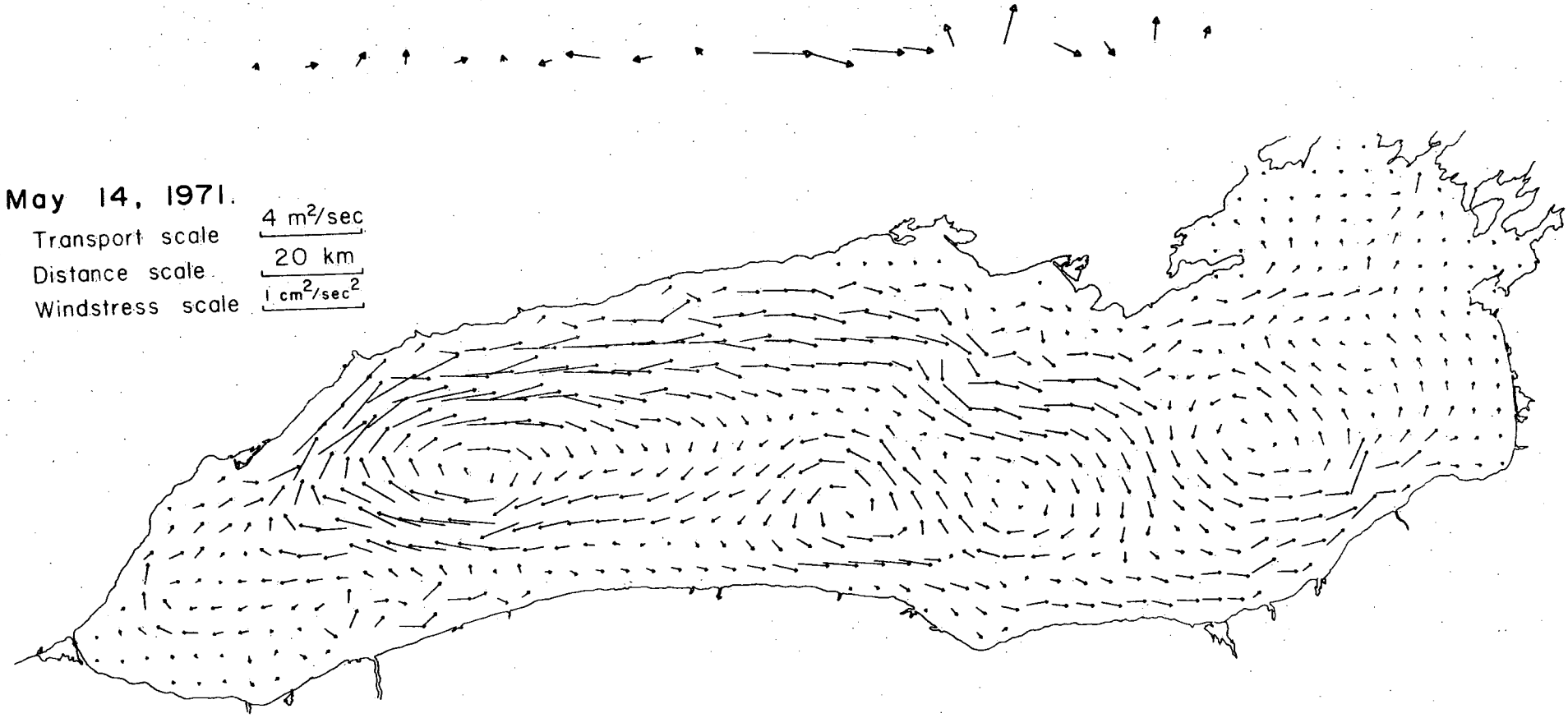
May 14, 1971.
Transport scale 4 m²/sec
Distance scale 20 km
Windstress scale 1 cm²/sec²

Figure 5.12

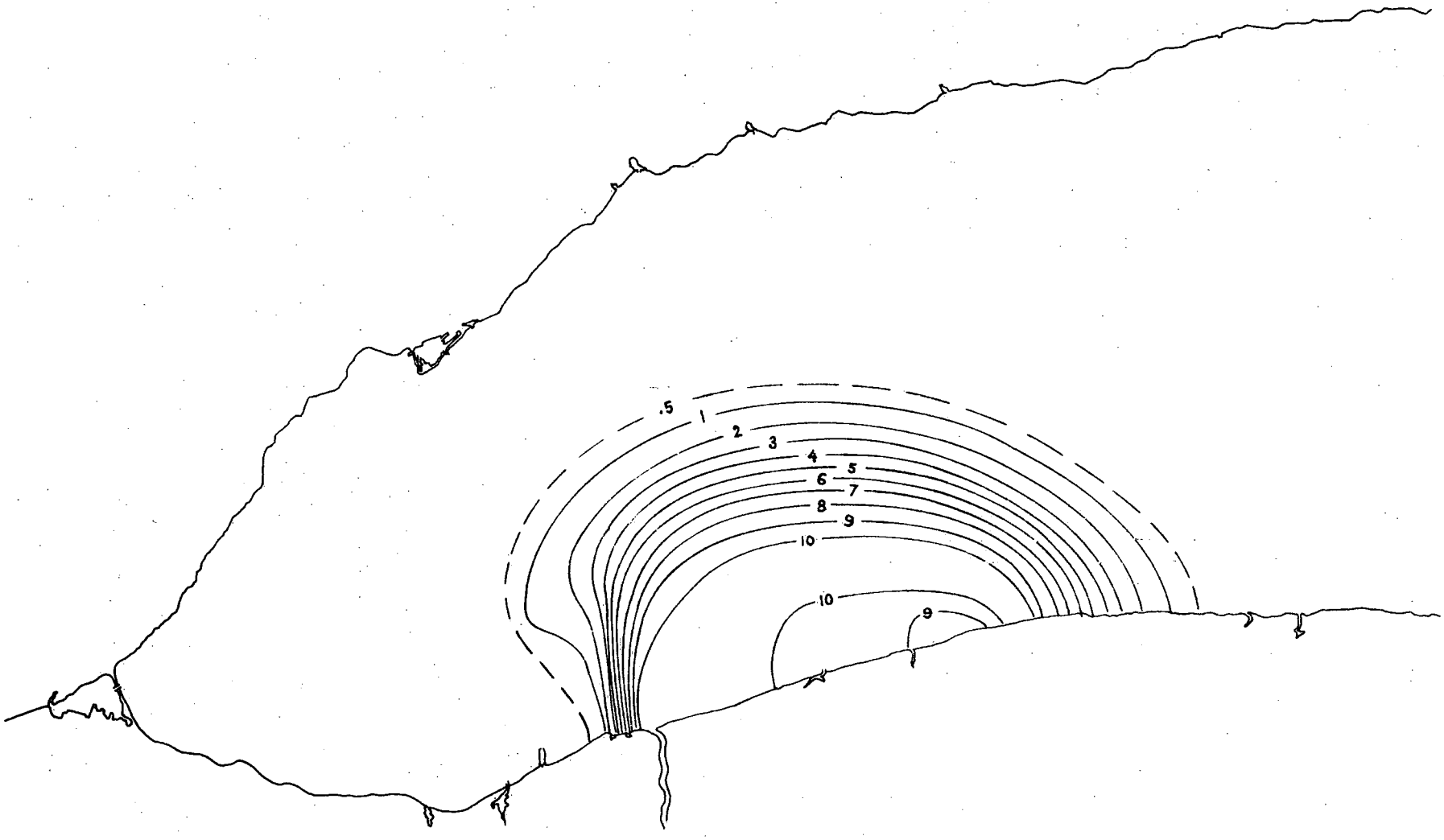

Figure 6.1

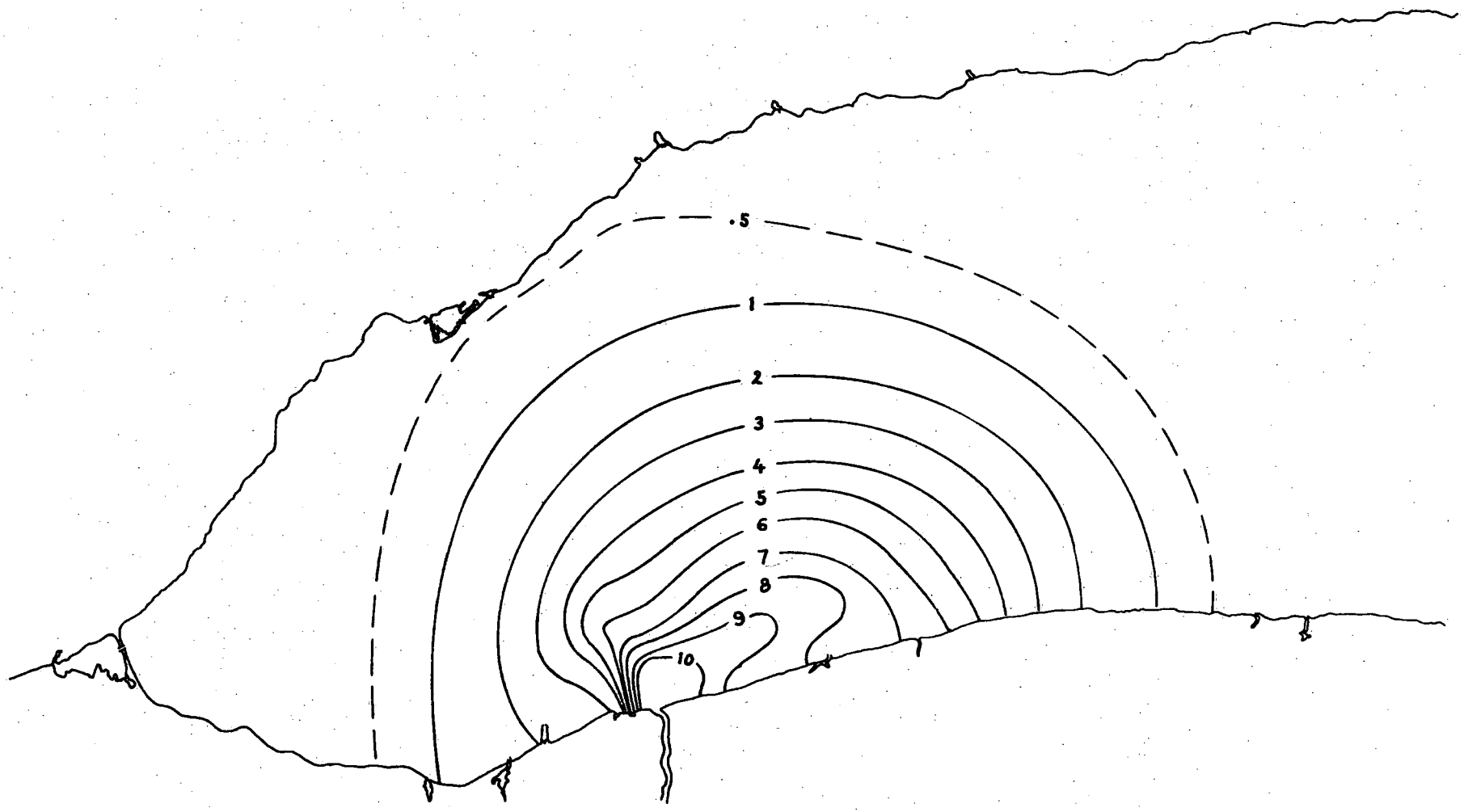

Figure 6.2

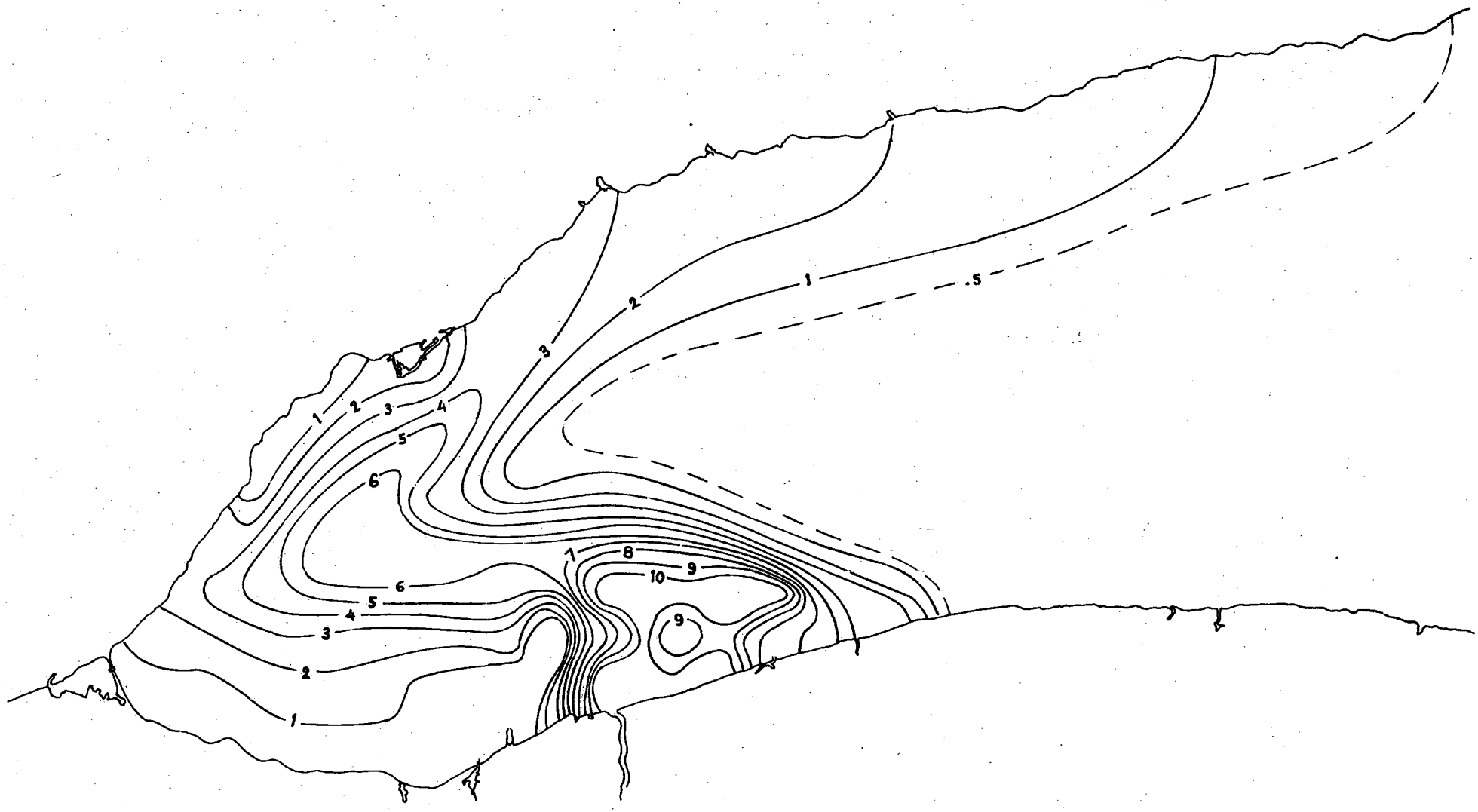

Figure 7.1

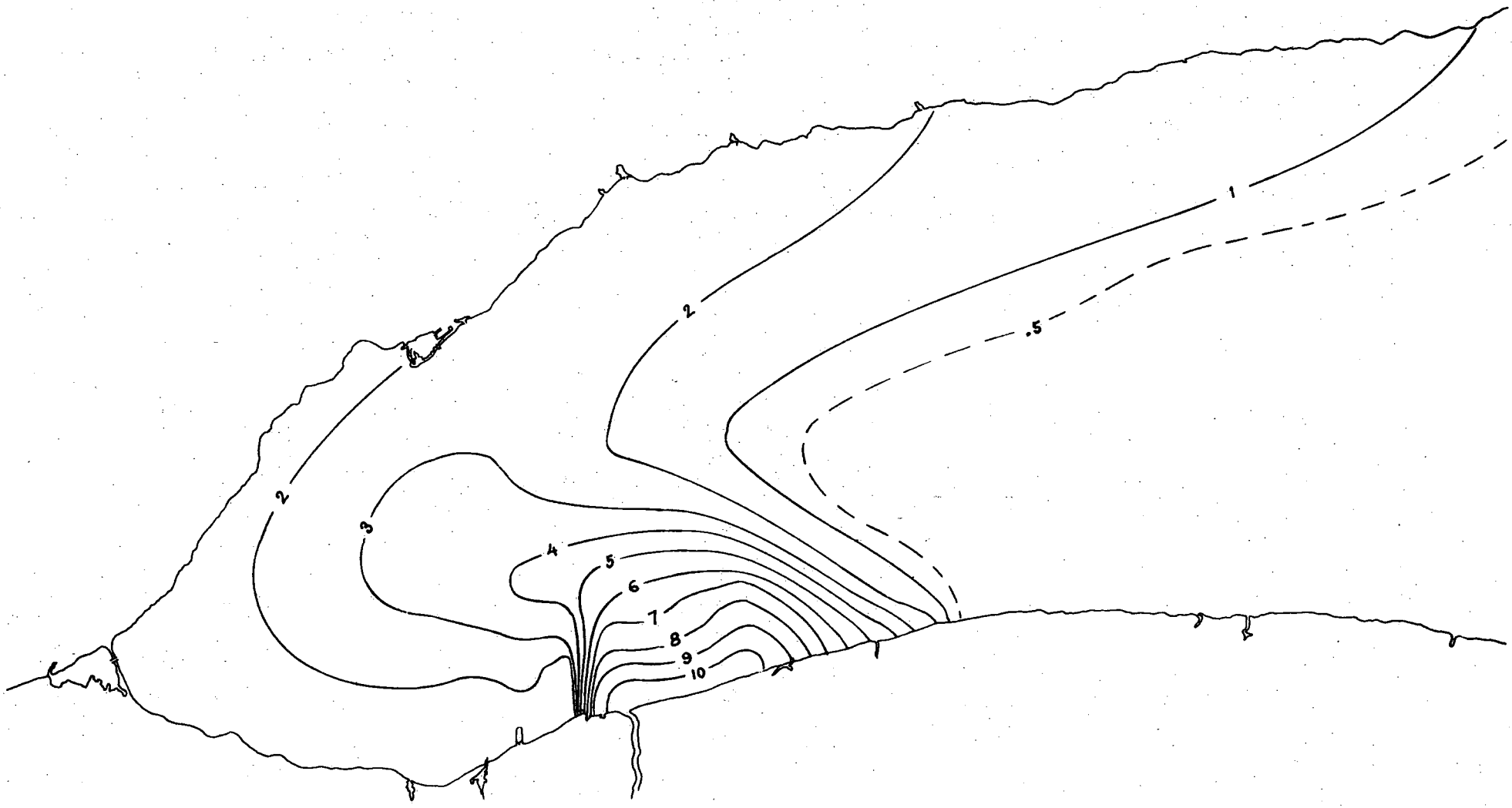

Figure 7.2

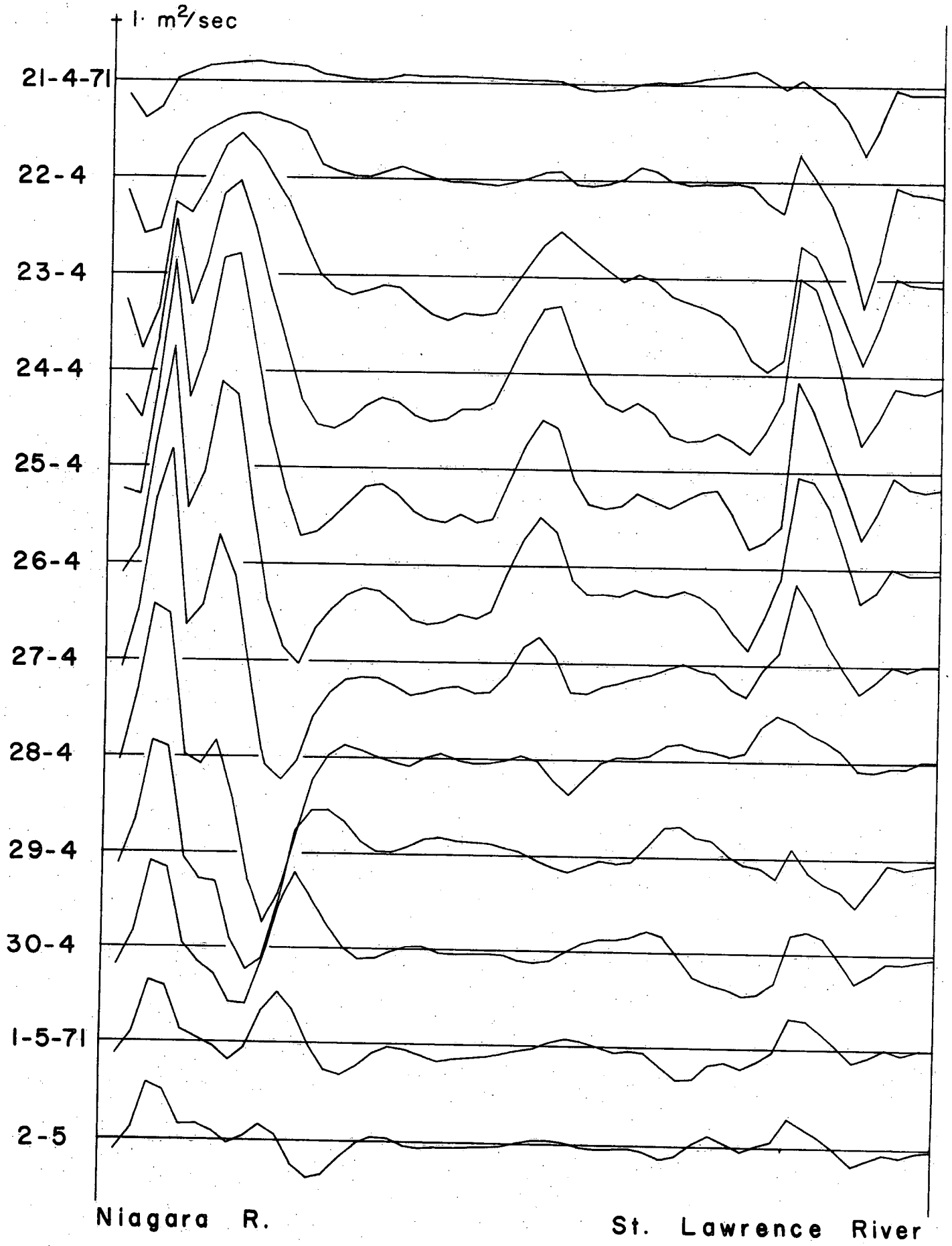
+1· m²/sec
21-4-71
22-4
23-4
24-4
25-4
26-4
27-4
28-4
29-4
30-4
1-5-71
2-5
Niagara R.
St. Lawrence River

Figure 8.1

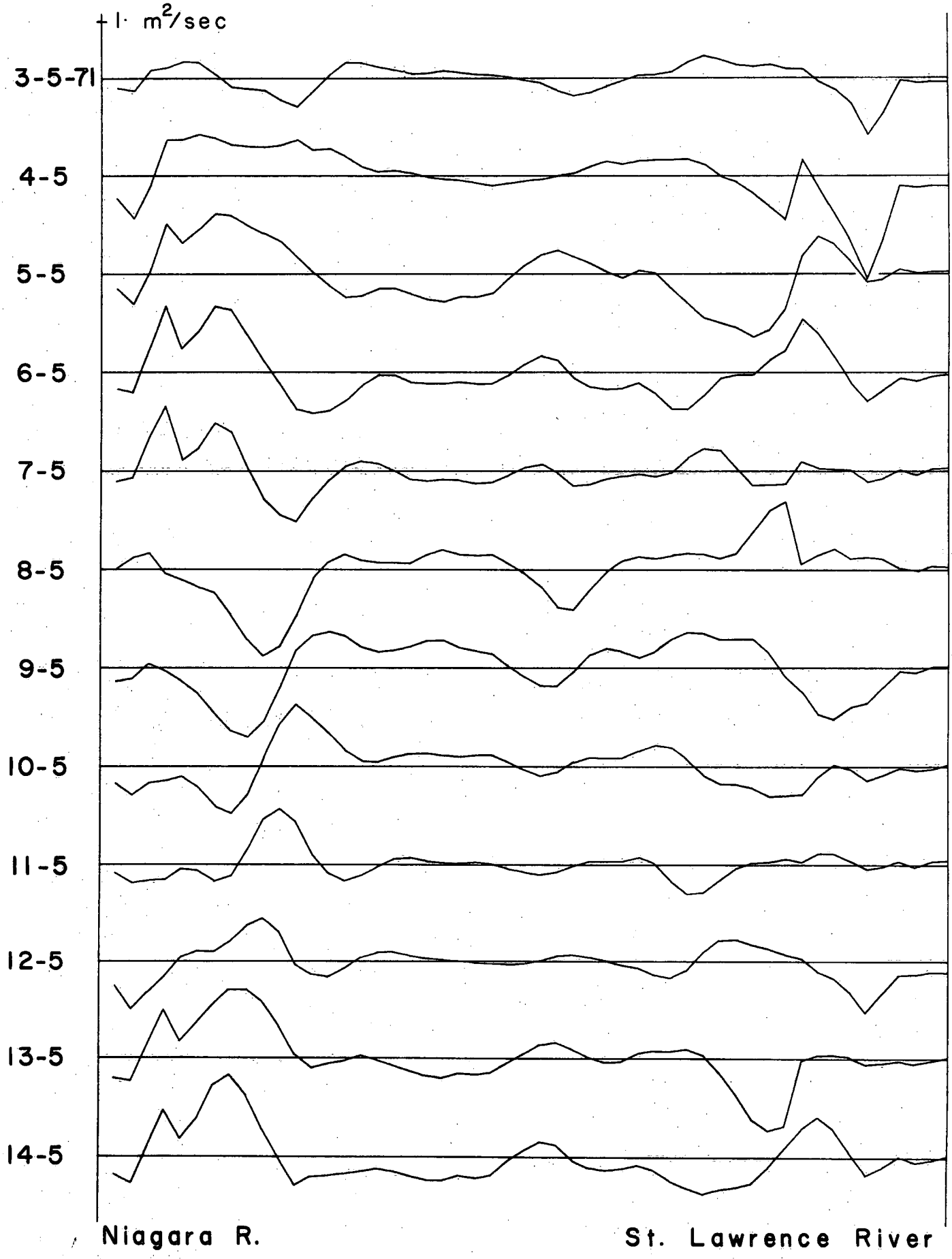
+1· m²/sec
3-5-71
4-5
5-5
6-5
7-5
8-5
9-5
10-5
11-5
12-5
13-5
14-5
Niagara R.
St. Lawrence River

Figure 8.2